Received: 22 December 2020 | Revised: 26 May 2021 | Accepted: 9 June 2021

IET Generation, Transmission & Distribution

DOI: 10.1049/gtd2.12236

The Institution of Engineering and Technology WILEY

ORIGINAL RESEARCH PAPER

Metrics and quantification of power-line and pipeline resiliency in integrated gas and power systems

Maosheng Sang[1] | **Yi Ding**[1] | **Ming Ding**[2] | **Minglei Bao**[1] | **Peng Wang**[3] | **Lei Sun**[2]

[1] College of Electrical Engineering, Zhejiang University, Hangzhou, China

[2] School of Electrical Engineering and Automation, Hefei University of Technology, Hefei, China

[3] School of Electrical and Electronic Engineering, Nanyang Technological University, Singapore, Singapore

Correspondence
Yi Ding, College of Electrical Engineering, Zhejiang University, Hangzhou 310027, China.
Email: yiding@zju.edu.cn

Funding information
National Natural Science Foundation of China, Grant/Award Number: 71871200

Abstract

Due to the increasing interactions between the natural gas system (NGS) and electric power system (EPS), the failures of power-lines or gas pipelines in one system may influence another system and consequently trigger widespread disruptions. Hence, identifying these critical components and protecting them from malfunctions are essential to prevent the collapse of integrated gas and power systems (IGPSs). Considering the effects of both network topologies and operational features on the resiliency evaluation, a novel assessment framework is proposed in this paper to screen out critical power-lines and gas pipelines. First, the framework of IGPSs is introduced and an optimal energy flow (OEF) model is constructed to quickly obtain the operation states under various disturbances. Furthermore, the resiliency metrics (RMs) are developed from structural and operational perspectives respectively. Specifically, structural RMs consider the coupling topologies to capture the structure-related resiliency, while operational RMs analyse the resiliency related to gas and power flow to capture physical operation characteristics. Finally, an assessment algorithm synthesizing all the metrics is proposed to quantify the comprehensive resiliency, based on which critical power-lines and pipelines (CPPs) can be detected. The effectiveness of the proposed approach is validated by an IGPS test system.

1 | INTRODUCTION

Over the past few decades, the proportion of natural gas power generation has extremely increased due to operation flexibilities and environmental benefits of gas-fired units (GFUs). Meanwhile, several electricity-driven facilities are adopted in natural gas systems (NGSs) whose electricity supplies are from electric power systems (EPSs) [1]. The deployment of GFUs and electricity-driven equipment greatly intensifies the interactions between NGSs and EPSs. To this end, any disturbance in one system induced by outages of some critical components could spread to the other one, and consequently cause catastrophic disruptions to the whole system. A dramatic real-world example is the electrical blackout that affected much of Texas on February 15, 2021: the outage of gas infrastructure such as pipelines and gas wells caused by the extreme cold weather directly led to the interrupted gas supplies for GFUs, which caused the further breakdown of power stations. More than 4.8 million consumers were seriously affected [2, 3]. Therefore, it is of great significance to identify these critical components and protect them from malfunctions to prevent the collapse of systems.

Generally, the resiliency of one component refers to the functionality degradation degree of the system when the component is out of service [4]. In integrated gas and power systems (IGPSs), the failure of generating units or substations is less frequent than that of transmission line outages, and the possibility of gas node malfunction is also much smaller than that of pipeline failures [5]. Hence, in this paper, the components with respect to the resiliency analysis of IGPSs mainly refer to the power-lines and pipelines. Moreover, the power-lines and pipelines with high resiliency are regarded as critical power-lines and pipelines (CPPs). For instance, the outages of critical pipelines could cause the interruption of gas fuels supplied to GFUs, consequently reducing the generating capacity of EPS [6]. The tripping of critical power-lines could lead to the interruption of power supplied to NGS, causing the

malfunction of electricity-driven gas sources (EDGSs) [7]. Under this background, it is in urgent need to quantify the resiliency of power-lines and pipelines and find out CPPs for preventing IGPSs from tremendous disruptions under unexpected disruptive events or deliberate attacks.

In previous studies, the resiliency assessment has been carried out extensively for engineering systems, such as transportation systems [8], power systems [9–12], and natural gas systems [13]. In [8, 10], the resiliency of transportation systems and power grids is analysed respectively from the perspective of network topology. In [9, 11], the framework of power grid resiliency assessment is proposed during extreme events, such as wildfire and high wind. In [12], a hybrid approach is developed for evaluating the power system resiliency by incorporating the topological analysis and reliability metrics. Besides, numerous efforts have been devoted to assessing the resiliency or vulnerability from the component-level point based on various methods, such as graph theory [8, 10–14], fault chain theory [15], entropy theory [16] and so on. The proposed techniques can be classified into two categories: structure topology-based methods and operation analysis-based methods. The first category mainly takes into account the topological characteristics of networks combined with physical properties, such as admittance or power flow of power-lines and energy supply reliability, then establishes structure-related resiliency metrics (RMs) [17]. In [18], a weighted betweenness based on the shortest electrical path is presented. In [19], an improved maximum flow approach is used to assess the structural resiliency or vulnerability of power systems. In [20], the cascading outages are modelled as the fault graph by which the power-line resiliency is converted into the corresponding topological importance in the graph, and then metrics such as degree and betweenness can be developed. In [13] the element importance of NGSs is analysed from the topological perspective. However, pure structural metrics may not correctly reflect the resiliency due to neglecting system operation characteristics. The vulnerability or resiliency of components may change significantly under different operation states despite being in the same topological structure [4].

As a result, to bridge the above gap, the second category methods utilizing operation analysis tools are proposed for resiliency evaluation. In [21, 22], several RMs based on numerical simulations of cascading failure are put forward. In [23], both static (via optimal power flow) vulnerability and dynamic (via transient stability) vulnerability of power networks are assessed considering load uncertainties. In [16], the concept of power flow entropy is defined to describe the distribution characteristics of power flow, then the operational RMs are constructed by incorporating the power flow entropy. Nevertheless, these metrics are developed based on the independent operation of power systems or natural gas systems, without considering the integration and interdependency with each other, such as IGPSs. To investigate the impact of ever-increasing interdependence between NGS and EPS, several studies have been conducted focused on the reliability and security problems of IGPSs. In [7], the interdependence-induced cascading effects are considered in the nodal reliability evaluation of IGPSs, but the operation of NGS and EPS is still optimized separately. In [24, 25], the long-term and short-term reliability of IGPSs are analysed respectively based on integrated optimal energy flow techniques, but the resiliency of components has not been deeply studied. In [26], the vulnerable components of NGSs and IGPSs are analysed from the structural perspective, but the operation properties such as energy flow redistribution under disturbances are not considered. Besides, the components concerning the resiliency analysis focus on nodes in the network, without analysing the links such as power-lines and pipelines that are more likely to fail in reality [5]. Therefore, the framework with a set of key metrics for joint resiliency assessment of pipelines and power-lines in IGPSs is seldom addressed in the literature.

It is worth emphasizing that the integration of NGSs and EPSs would pose new challenges to the resiliency assessment. On one hand, due to the interdependences of EPSs and NGSs, more factors need to be considered for metric construction compared with individual systems, such as the coupling network topologies and operation interactions. On the other hand, allowing for different structural characteristics and operation properties, the metrics for power-lines and pipelines should be distinct. Moreover, owing to the complexity and diversity of metrics, it is more difficult to establish a reasonable and effective evaluation algorithm to synthesize these metrics. To tackle the above challenges, this paper proposes a novel method for quantifying the resiliency of power-lines and pipelines in IGPSs. The main contributions are summarized as follows:

1. Metrics in terms of structural and operational integrity are introduced to quantify the resiliency of power-lines and pipelines in IGPSs. In specific, structural RMs considering the coupling topologies are constructed based on the complex network theory to capture the structure-related resiliency, while operational RMs are established to analyse the resiliency related to energy flows under various disturbances.
2. An optimal energy flow (OEF) model is constructed to determine the operation states of IGPSs under various disturbance scenarios such as power-line and pipeline outages. Moreover, the model is transformed into mixed-integer linear programming by utilizing linearization techniques to relieve the computation burden considerably.
3. An assessment algorithm is proposed to synthesize all the metrics to quantify the comprehensive resiliency and identify CPPs. Specifically, the optimal combination weight (OCW) is utilized to determine the weight of each metric integrating both subjective and objective weighting methods, and the technique for order preference by similarity to an ideal solution (TOPSIS) method is improved to quantify the comprehensive resiliency.

The remainder of this paper is organized as follows. In Section 2, the structure and operation model of IGPSs are introduced. The multi-dimensional resiliency metrics are developed in Section 3. The assessment algorithm synthesizing all the metrics to quantify the comprehensive resiliency and detect critical power-lines and pipelines is proposed in Section 4. Case

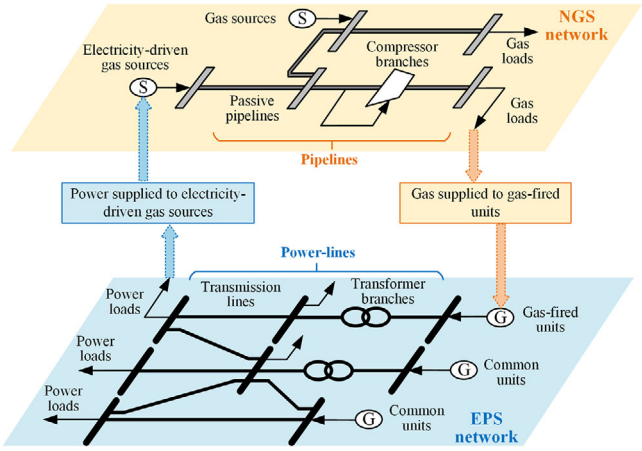

FIGURE 1 Structure of integrated gas and power systems

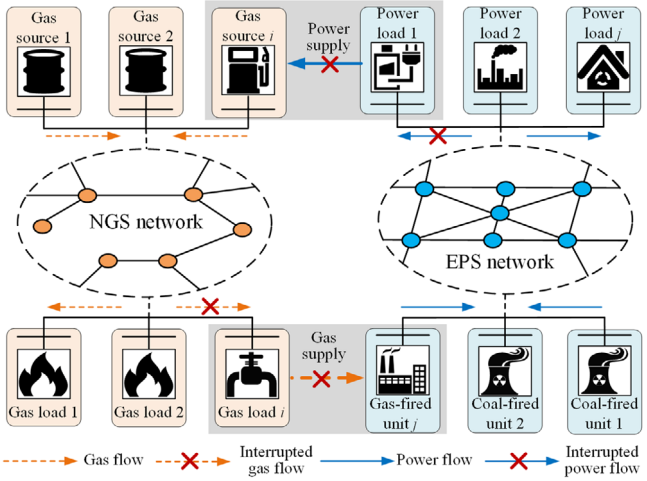

FIGURE 2 Illustration of failure propagation within IGPSs

studies are carried out in Section 5 and the conclusions are given in Section 6.

2 | DESCRIPTION OF INTEGRATED GAS AND POWER SYSTEMS

2.1 | Structural framework for IGPSs

The described IGPSs consist of NGS and EPS, as shown in Figure 1, which can be depicted as the combination of two networks: NGS network and EPS network. The NGS network is comprised of gas nodes that represent gas sources (gas wells) or gas loads. The gas nodes are connected by gas pipelines including gas passive pipelines and compressor branches (or active pipelines). The EPS network consists of electric nodes representing generating units or electric loads. The electric nodes are connected by power-lines such as transmission lines and transformer branches. The NGS network and EPS network are integrated through coupling infrastructures, including GFUs and EDGSs.

The gas flow produced by gas wells is transmitted to gas loads by gas pipelines and the power flow produced by generating units is transmitted to power loads by power-lines. Meanwhile, the gas flow transmitted from NGS is supplied to GFUs for electricity generation and the power flow in EPS is supplied to EDGSs to maintain the normal operation.

2.2 | Failure propagation within IGPSs

As shown in Figure 1, the ever-increasing interdependence of NGS and EPS could lead to a wider range of failure propagation in IGPSs. In specific, the outages of power-lines would not only affect the operation of EPS but also influence the operation of NGS. As shown in Figure 2, the EDGSs are inevitably shut down due to the interrupted power flow when some power-lines trip, further leading to the redistribution of gas flow and gas demand curtailments in the NGS. Moreover, the pipeline failure affects the NGS and EPS simultaneously. The generating capacity of GFUs would be reduced because of the interruption of gas fuels when some pipelines malfunction as shown in Figure 2, causing the transfer of power flow and load shedding in EPS.

As a result, the resiliency assessment for IGPSs should take into account the interdependence between the EPS and NGS. Of note, considering the node failure is less frequent than transmission line outages and pipeline failures in IGPSs [5], the components for the resiliency analysis in this paper mainly refer to power-lines and pipelines.

2.3 | Optimal energy flow model

One of the important issues before resiliency assessment is to determine the operation states of IGPSs under various disturbance scenarios, such as the power-line tripping and pipeline outages. To this end, a scenario-based OEF model is developed by jointly optimizing the operation states of the EPS and NGS. The objective is to minimize the operation cost of IGPSs, that is, the sum of production cost and load shedding cost for NGS and EPS.

$$\min \quad \sum_{i\in I} C_i^l\left(F_{\text{sour},i}^l, F_{\text{LS},i}^l\right) + \sum_{j\in J} C_j^l\left(P_{\text{gen},j}^l, P_{\text{GFU},j}^l, P_{\text{LS},j}^l\right) \tag{1}$$

Subject to the following NGS operation constraints (2)–(9), EPS operation constraints (10)–(16), and coupling constraints (17)–(20).

The gas flow balance equation at gas node i:

$$F_{\text{sour},i}^l - F_{\text{load},i} - F_{\text{GFU},i}^l + F_{\text{LS},i}^l = \sum_{p_g\in P_{g1}(i)} f_{p_g}^l + \sum_{p_c\in P_{c1}(i)} \tau_{p_c}^l - \sum_{p_g\in P_{g2}(i)} f_{p_g}^l - \sum_{p_c\in P_{c2}(i)} \tau_{p_c}^l \tag{2}$$

The relationship between gas flow and node pressures for passive pipelines satisfies Weymouth equation [27]:

$$f_{p_g}^l \left| f_{p_g}^l \right| = M_{p_g}^2 \left(\pi_{p_{g1}}^l - \pi_{p_{g2}}^l \right) \tag{3}$$

The relationship between gas flow and node pressures for compressor branches:

$$\tau_{p_c}^l \left| \tau_{p_c}^l \right| \geq M_{p_c}^2 \left(\pi_{p_{c1}}^l - \pi_{p_{c2}}^l \right), \quad \tau_{p_c}^l \geq 0 \tag{4}$$

The gas variable constraints:

$$y_{\text{sour},i}^l F_{\text{sour},i}^{\min} \leq F_{\text{sour},i}^l \leq y_{\text{sour},i}^l F_{\text{sour},i}^{\max} \tag{5}$$

$$f_{p_g}^{\min} \leq f_{p_g}^l \leq f_{p_g}^{\max} \tag{6}$$

$$\pi_i^{\min} \leq \pi_i^l \leq \pi_i^{\max} \tag{7}$$

$$\pi_{p_{c2}}^l \left(\gamma_{p_c}^{\min} \right)^2 \leq \pi_{p_{c1}}^l \leq \left(\gamma_{p_c}^{\max} \right)^2 \pi_{p_{c2}}^l \tag{8}$$

$$0 \leq F_{\text{LS},i}^l \leq F_{\text{load},i} \tag{9}$$

The power flow balance equation at EPS node j:

$$P_{\text{gen},j}^l + P_{\text{GFU},j}^l - P_{\text{load},j} + P_{\text{LS},j}^l = \sum_{k \in K_1(j)} pf_k^l - \sum_{k \in K_2(j)} pf_k^l \tag{10}$$

The relationship between power flow and phase angle:

$$pf_k^l = (\theta_{k1}^l - \theta_{k2}^l)/x_k \tag{11}$$

The electric variable constraints:

$$P_{\text{GFU},j}^{\min} \leq P_{\text{GFU},j}^l \leq P_{\text{GFU},j}^{\max} \tag{12}$$

$$P_{\text{gen},j}^{\min} \leq P_{\text{gen},j}^l \leq P_{\text{gen},j}^{\max} \tag{13}$$

$$-pf_k^{\max} \leq pf_k^l \leq pf_k^{\max} \tag{14}$$

$$\theta_j^{\min} \leq \theta_j^l \leq \theta_j^{\max} \tag{15}$$

$$0 \leq P_{\text{LS},j}^l \leq P_{\text{load},j} \tag{16}$$

For GFUs, the conversion relationship between gas consumption and power output can be expressed as:

$$P_{\text{GFU},j}^l \big|_{j \to i} = \eta_{\text{G2P}} F_{\text{GFU},i}^l G_{HV} \tag{17}$$

where $j \to i$ means that the GFUs at electric node j are connected to gas node i.

For EDGSs, the normal operation depends on the power supply of the connected electrical nodes. If the power supply is lower than a certain value, which is related to the amount of gas production, the gas sources would be shut down [1]. So the operational constraints of EDGSs can be expressed as:

$$y_{\text{sour},i}^l = \begin{cases} 1 & P_{\text{load},j} - P_{\text{LS},j}^l > \eta_{\text{P2G}} F_{\text{sour},i}^{\max} \big|_{i \to j} \\ 0 & P_{\text{load},j} - P_{\text{LS},j}^l \leq \eta_{\text{P2G}} F_{\text{sour},i}^{\max} \big|_{i \to j} \end{cases} \tag{18}$$

All formulas in the above OEF model (1)–(18) are linear except for Weymouth Equations (3)–(4) and the operation constraint of EDGSs in Equation (18). The Weymouth equations can be linearized by utilizing piecewise linearization approximation [28]. Moreover, the linear representations of Equation (18) can be given as Equations (19)–(20) by introducing auxiliary binary variable $z_{\text{sour},i}^l$.

$$z_{\text{sour},i}^l - 1 \leq 1 - y_{\text{sour},i}^l \leq z_{\text{sour},i}^l \tag{19}$$

$$z_{\text{sour},i}^l = \left(P_{\text{LS},j}^l + \eta_{\text{P2G}} F_{\text{sour},i}^{\max} \big|_{i \to j} \right) \Big/ P_{\text{load},j} \tag{20}$$

where $i \to j$ means that the EDGSs at i is connected to j. $z_{\text{sour},i}^l$ is an auxiliary continuous variable and calculated as Equation (20). Equations (19), (20) denote that if the load curtailment is not less than the threshold value, i.e. $P_{\text{LS},j}^l \geq P_{\text{load},j} - \eta_{\text{P2G}} F_{\text{sour},i|i \to j}^{\max}$, then $z_{\text{sour},i}^l \geq 1$ and $y_{\text{sour},i}^l = 0$, that is, the gas source would be shut down; otherwise, $P_{\text{LS},j}^l < P_{\text{load},j} - \eta_{\text{P2G}} F_{\text{sour},i|i \to j}^{\max}$, $z_{\text{sour},i}^l < 1$ and $y_{\text{sour},i}^l = 1$.

By utilizing the piecewise linearization approximation technique and the linear representations of constraint (18) as Equations (19)–(20), the OEF model can be transformed into a mixed-integer linear programming problem, which can be solved quickly by commercial software such as CPLEX. It should be noted that the established OEF model can be utilized to determine the operating states of IGPSs under both normal and various disturbance scenarios (i.e. outages of pipelines or power-lines). For instance, if one power-line fails, it can be removed from the network topology of IGPSs, then the OEF model can be used to determine the operating states under the updated network topology. The operation states include the energy flow (i.e. power flow and gas flow) through each pipeline and power-line, the gas and electricity load curtailment at each load node, which can be used as input to the calculation of RMs proposed in the next section.

3 | MULTI-DIMENSIONAL RESILIENCY METRICS

The multi-dimensional RMs are developed in this section considering both topological structure and system operation states

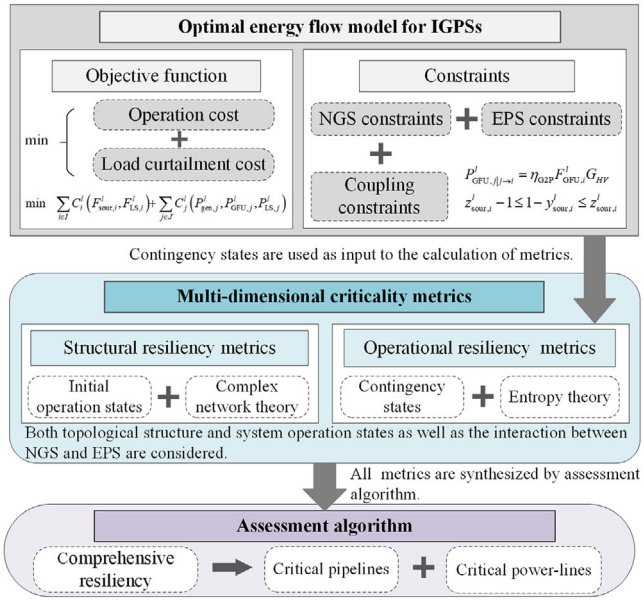

FIGURE 3 Framework for resiliency assessment of power-lines and pipelines

as well as the interaction between NGS and EPS. As shown in Figure 3, the structural RMs are first constructed based on the complex network theory considering the initial operating states of IGPSs. Meanwhile, the operational RMs are established to quantify the resiliency related to the energy flow under contingency states. To compute RMs, the OEF model developed in Section 2.3 is utilized to determine the operating states of IGPSs under various scenarios. Finally, the assessment algorithm synthesizing all the RMs is proposed in the next section to quantify the comprehensive resiliency, based on which critical power-lines and pipelines (CPPs) can be detected.

3.1 | Structural RMs for pipelines

3.1.1 | Gas betweenness centrality

In the complex network theory, the betweenness centrality of an edge is described by the number of shortest paths through the edge [19], which is calculated as:

$$BC_\alpha = \sum_{s \neq t} \frac{n_{s,t}(\alpha)}{g_{s,t}} \tag{21}$$

where $g_{s,t}$ refers to the number of shortest paths from node s to node t; $n_{s,t}(\alpha)$ refers to the number of shortest paths through edge α in $g_{s,t}$.

The betweenness centrality metric BC_α describes the ability of an edge to control the transmission capacity of the network. The larger the betweenness centrality, the greater the impact on the transmission capacity of the network after removing the edge, and the more critical the edge is. Therefore, the betweenness centrality is commonly utilized to reflect the importance of an edge in the network in terms of topological structure.

However, the metric BC_α in Equation (21) cannot be directly applied to the component resiliency assessment of IGPSs since it fails to take the physical operation characteristics into account. On one hand, it considers that the length of all edges is the same when searching for the shortest paths between node pairs, while the length of edges in IGPSs is different due to distinct parameter values, such as transmission coefficient M_p for pipelines and reactance x_k for power-lines. On the other hand, the metric BC_α neglects the weights of each node pair and path, but the weights are different depending on the amount of carried energy flow.

To compensate for the above deficiencies, the gas betweenness centrality (GBC) for pipelines is defined by modifying BC_α as

$$GBC_p = \frac{\sum_{i \neq i' \in I} \sum_{m \in \mathbb{C}_{i,i'}} \omega_{i,i'} \sigma^m_{i,i'} \zeta^m_{i,i'}(p)}{\sum_{i \neq i' \in I'} \sum_{m \in \mathbb{C}_{i,i'}} \omega_{i,i'} \sigma^m_{i,i'}} \tag{22}$$

where $\omega_{i,i'}$ refers to the weight of node pair between i and i' and can be calculated as (23). $\sigma^m_{i,i'}$ is the weight of the m-th shortest path between node i and i' and equal to the minimum transmission capacity of pipelines contained. It is worthwhile to mention that the reciprocal of pipeline transmission coefficient $1/M_p$ is taken as the pipeline's length when calculating the shortest path between node i and i', since the gas flow through pipelines is proportional to M_p according to Weymouth equation [27] and Equation (3). Specifically, the larger the M_p for pipeline p, the larger the gas flow through it, and the smaller the pipeline's length.

$$\omega_{i,i'} = \min\left(F^{l_0}_{\text{sour},i}, F_{\text{load},i'} + F^{l_0}_{\text{GFU},i'}\right) \tag{23}$$

As shown in Equations (22) and (23), the GBC_p considers the transmission properties of pipelines and gas flow in IGPSs such as the gas production of gas wells and gas consumptions of loads. The larger the GBC_p, the greater the impact on the transmission capacity of the gas network after removing the pipeline, and the more critical the pipeline is.

3.1.2 | Gas degree centrality

In the complex network theory, the degree centrality [29] of a node is computed by the number of adjacent nodes. The large degree means the great importance of the node on the network. Because the conventional degree centrality metric fails to consider the physical operation characteristics of IGPSs, the gas degree centrality (GDC) for gas nodes is defined as

$$GDC_i = \frac{\sum_{p \in P(i)} f^{\max}_p + F^{l_0}_{\text{sour},i} + F^{l_0}_{\text{GFU},i} + F_{\text{load},i}}{2} \tag{24}$$

Based on the GDC_i for gas nodes, the GDC metric for pipelines is calculated by averaging the GDC_i of nodes at both sides of the pipeline:

$$GDC_p = \frac{GDC_{p_1} + GDC_{p_2}}{2} \tag{25}$$

As shown in Equations (24) and (25), the GDC_i for gas nodes and GDC_p for pipelines consider the transmission capacity of pipelines as well as gas flow in IGPSs. The larger the GDC_p, the greater the impact on the transmission capacity of adjacent nodes after removing the pipeline, and the more critical the pipeline is.

It is worth noting that although both GBC_p and GDC_p metrics describe the resiliency of pipelines in terms of topological structure, they are not the same. The GBC_p characterizes the global importance of pipeline in the network, while the GDC_p is to depict the local importance of pipelines related to adjacent nodes.

3.2 | Structural RMs for power-lines

3.2.1 | Electrical betweenness centrality

Similar to the GBC_p metric for pipelines, the electrical betweenness centrality (EBC) for power-lines is defined as

$$EBC_k = \frac{\sum_{j \neq j' \in J} \sum_{n \in \mathbb{Z}_{j,j'}} \varpi_{j,j'} \partial^n_{j,j'} \zeta^n_{j,j'}(k)}{\sum_{j \neq j' \in J} \sum_{n \in \mathbb{Z}_{j,j'}} \varpi_{j,j'} \partial^n_{j,j'}} \tag{26}$$

where $\varpi_{j,j'}$ refers to the weight of node pair between node j and j' and can be calculated as (27). $\partial^n_{j,j'}$ is the weight of the n-th shortest path between node j and j' and equal to the minimum transmission capacity of power-lines contained; $i \to j'$ means that the EDGSs at gas node i is connected to electric node j'. It is worthwhile to mention that the reactance of power-line x_k is taken as the power-line's length when searching for the shortest path between node j and j', since the power flow through power-lines is inversely proportional to x_k according to Equation (11). Specifically, the larger the x_k for power-line k, the smaller the power flow through it, and the larger the power-line's length.

$$\varpi_{j,j'} = \min\left(P^{\prime 0}_{\text{gen},j} + P^{\prime 0}_{\text{GFU},j}, P_{\text{load},j'} + \eta_{\text{P2G}} F^{\max}_{\text{sour},i|i \to j'}\right) \tag{27}$$

As shown in Equations (26) and (27), the EBC_k considers the transmission properties of power-lines and power flow in IGPSs such as the electricity generation of common generating units and GFUs and power loads. The larger the EBC_k, the greater the impact on the transmission capacity of the power network after removing the power-line, and the more critical the power-line is.

3.2.2 | Electrical degree centrality

Similar to the GDC_p metric for pipelines, the electrical degree centrality (EDC) for power-lines is defined by:

$$EDC_k = \frac{EDC_{k_1} + EDC_{k_2}}{2} \tag{28}$$

where EDC_{k1} and EDC_{k2} refer to EDC metric for electric nodes at both sides of power-line k, which can be calculated by Equation (29).

$$EDC_j = \frac{\sum_{k \in K(j)} p f^{\max}_k + P^{\prime 0}_{\text{gen},j} + P^{\prime 0}_{\text{GFU},j} + P_{\text{load},j}}{2} \tag{29}$$

As shown in Equations (28) and (29), the EDC_j for electric nodes and EDC_k for power-lines consider the transmission capacity of power-lines as well as power flow in IGPSs. The larger the EDC_k, the greater the impact on the transmission capacity of adjacent nodes after removing the power-line, and the more critical the power-line is.

It is worth noting that EBC_k and EDC_k metrics describe the resiliency of power-lines from different perspectives. The EBC_k characterizes the global importance of power-lines in the network, while the EDC_k is to depict the local importance of power-lines related to adjacent nodes.

3.3 | Operational RMs for pipelines and power-lines

In Sections 3.1 and 3.2, the structural RMs for pipelines and power-lines are established respectively to describe the resiliency in terms of topological structure based on the normal operation states. Nevertheless, the operation states of IGPSs could change from normal states to various contingency states with the occurrence of pipeline outages or power-line tripping, which has a significant impact on the resiliency of components. Therefore, the operational RMs for pipelines and power-lines are developed in this subsection to reflect the resiliency related to energy flow.

3.3.1 | Energy flow transfer entropy

In EPS, when a power-line fails, the power flow through it will be redistributed to other power-lines, which may cause the overload of some other power-lines and even lead to cascading failures. The uneven degree of power flow redistribution caused by the failure of distinct power-lines is different. In [16], the power flow entropy is proposed to measure the diversity of the load distribution in the network. Nevertheless, it does not consider the power flow redistribution caused by failure disturbances, such as power-line failures. To characterize the uneven degree of power flow redistribution when a

power-line is broken, the power flow transfer entropy (PFTE) is proposed as:

$$\mathfrak{R}_k^{\mathrm{ee}} = -\sum_{k' \in K} \eta_{k',k} \ln \eta_{k',k} \tag{30}$$

where $\mathfrak{R}_k^{\mathrm{ee}}$ is the PFTE caused by the malfunction of power-line k. $\eta_{k',k}$ is the power flow impact ratio on power-line k' caused by the malfunction of power-line k and can be calculated by Equation (31).

$$\eta_{k',k} = \frac{\Delta p f_{\mathrm{line},k'}^{k}}{\sum_{k' \in K} \Delta p f_{\mathrm{line},k'}^{k}} \tag{31}$$

where $\Delta p f_{\mathrm{line},k'}^{k}$ is the incremental power flow of power-line k' caused by the malfunction of power-line k and can be calculated by Equation (32). Considering the possibility of reverse flow, the scenario in which the absolute values of carried flow after component failures are larger than the initial values is considered when calculating $\Delta p f_{\mathrm{line},k'}^{k}$, and so are $\Delta f_{\mathrm{pipe},p'}^{k}$, $\Delta f_{\mathrm{pipe},p'}^{p}$ and $\Delta p f_{\mathrm{line},k'}^{p}$ in Equations (35), (42) and (43).

$$\Delta p f_{\mathrm{line},k'}^{k} = \begin{cases} \dfrac{\left| p f_{\mathrm{line},k'}^{k} - p f_{\mathrm{line},k'}^{0} \right|}{p f_{\mathrm{line},k'}^{\max} - p f_{\mathrm{line},k'}^{0}}, & \left| p f_{\mathrm{line},k'}^{k} \right| > \left| p f_{\mathrm{line},k'}^{0} \right| \\ 0 & \left| p f_{\mathrm{line},k'}^{k} \right| \le \left| p f_{\mathrm{line},k'}^{0} \right| \end{cases} \tag{32}$$

As shown in Equations (30)–(32), the $\mathfrak{R}_k^{\mathrm{ee}}$ measures the diversity of the power flow redistribution caused by the failure of power-line k. Two extreme cases are the maximal value and the minimal one. The maximum value is $\mathfrak{R}_k^{\mathrm{ee}} = \ln K$ when $\eta_{k',k} = \frac{1}{K}$, that is, the incremental power flow of all power-lines is the same. The minimal value is $\mathfrak{R}_k^{\mathrm{ee}} = 0$ when the incremental power flow is concentrated in only one power-line, which is very likely to cause the overload of other power-lines. As a result, the smaller the $\mathfrak{R}_k^{\mathrm{ee}}$, the more uneven the power flow redistribution after removing the power-line, and the more critical the power-line is.

Due to the interaction of EPS and NGS, the failure of power-lines may also influence the operation of NGS. For instance, the EDGSs are inevitably shut down due to the interrupted power flow when some power-lines trip, further leading to the redistribution of gas flow and demand curtailments in the NGS. In order to characterize the uneven degree of gas flow redistribution when a power-line is broken, the gas flow transfer entropy (GFTE) is proposed as

$$\mathfrak{R}_k^{\mathrm{eg}} = -\sum_{p' \in P} \eta_{p',k} \ln \eta_{p',k} \tag{33}$$

where $\mathfrak{R}_k^{\mathrm{eg}}$ is the GFTE caused by the malfunction of power-line k. $\eta_{p',k}$ is the gas flow impact ratio on pipeline p' caused by the malfunction of power-line k and can be calculated by Equation (34).

$$\eta_{p',k} = \frac{\Delta f_{\mathrm{pipe},p'}^{k}}{\sum_{p' \in P} \Delta f_{\mathrm{pipe},p'}^{k}} \tag{34}$$

where $\Delta f_{\mathrm{pipe},p'}^{k}$ is the incremental gas flow of pipeline p' caused by the malfunction of power-line k and can be calculated by Equation (35).

$$\Delta f_{\mathrm{pipe},p'}^{k} = \begin{cases} \dfrac{\left| f_{\mathrm{pipe},p'}^{k} - f_{\mathrm{pipe},p'}^{0} \right|}{f_{\mathrm{pipe},p'}^{\max} - f_{\mathrm{pipe},p'}^{0}}, & \left| f_{\mathrm{pipe},p'}^{k} \right| > \left| f_{\mathrm{pipe},p'}^{0} \right| \\ 0 & \left| f_{\mathrm{pipe},p'}^{k} \right| \le \left| f_{\mathrm{pipe},p'}^{0} \right| \end{cases} \tag{35}$$

Based on $\mathfrak{R}_k^{\mathrm{eg}}$ and $\mathfrak{R}_k^{\mathrm{eg}}$ as well as the initial power flow, the energy flow transfer entropy (EFTE) for power-lines can be defined as:

$$EFTE_k = p f_k^{l_0} \left(v \frac{1}{\mathfrak{R}_k^{\mathrm{ee}}} + (1 - v) \frac{1}{\mathfrak{R}_k^{\mathrm{eg}}} \right) \tag{36}$$

where v means the weight of power-line failure impact on EPS. An extreme case is $v = 1$, indicating that only the power flow redistribution is considered in the resiliency assessment of power-lines.

In the same way, the energy flow transfer entropy (EFTE) for pipelines can be defined as:

$$EFTE_p = f_p^{l_0} \left(u \frac{1}{\mathfrak{R}_p^{\mathrm{gg}}} + (1 - u) \frac{1}{\mathfrak{R}_p^{\mathrm{ge}}} \right) \tag{37}$$

where $\mathfrak{R}_k^{\mathrm{gg}}$ and $\mathfrak{R}_k^{\mathrm{ge}}$ are respectively the GFTE and PFTE caused by the malfunction of pipeline p, which are calculated by Equations (38) and (39). u refers to the weight of pipeline failure impact on NGS. An extreme case is $u = 1$, indicating that only the gas flow redistribution is considered in the resiliency assessment of pipelines.

$$\mathfrak{R}_p^{\mathrm{gg}} = -\sum_{p' \in P} \eta_{p',p} \ln \eta_{p',p} \tag{38}$$

$$\mathfrak{R}_p^{\mathrm{ge}} = -\sum_{k' \in K} \eta_{k',p} \ln \eta_{k',p} \tag{39}$$

where $\eta_{p',p}$ and $\eta_{k',p}$ are respectively the gas flow impact ratio on pipeline p' and power flow impact ratio on power-line k' caused by the malfunction of pipeline p, which are expressed as:

$$\eta_{p',p} = \frac{\Delta f_{\mathrm{pipe},p'}^{p}}{\sum_{p' \in P} \Delta f_{\mathrm{pipe},p'}^{p}} \tag{40}$$

$$\eta_{k',p} = \frac{\Delta p f_{\mathrm{line},k'}^{p}}{\sum_{k' \in K} \Delta p f_{\mathrm{line},k'}^{p}} \tag{41}$$

where $\Delta f^{p}_{\text{pipe},p'}$ and $\Delta pf^{p}_{\text{line},k'}$ are respectively the incremental gas flow of pipeline p' and incremental power flow of power-line k' caused by the malfunction of pipeline p.

$$\Delta f^{p}_{\text{pipe},p'} = \begin{cases} \dfrac{\left|f^{p}_{\text{pipe},p'} - f^{0}_{\text{pipe},p'}\right|}{f^{g}_{p'} - f^{0}_{\text{pipe},p'}}, & \left|f^{p}_{\text{pipe},p'}\right| > \left|f^{0}_{\text{pipe},p'}\right| \\ 0 & \left|f^{p}_{\text{pipe},p'}\right| \le \left|f^{0}_{\text{pipe},p'}\right| \end{cases} \tag{42}$$

$$\Delta pf^{p}_{\text{line},k'} = \begin{cases} \dfrac{\left|pf^{p}_{\text{line},k'} - pf^{0}_{\text{line},k'}\right|}{pf^{\max}_{\text{line},k'} - pf^{0}_{\text{line},k'}}, & \left|pf^{p}_{\text{line},k'}\right| > \left|pf^{0}_{\text{line},k'}\right| \\ 0 & \left|pf^{p}_{\text{line},k'}\right| \le \left|pf^{0}_{\text{line},k'}\right| \end{cases} \tag{43}$$

As shown in Equations (36) and (37), the $EFTE_k$ and $EFTE_p$ respectively reflect the disturbance degree of power-line failures and pipeline failures to energy flow redistribution. The larger the $EFTE_k$ and $EFTE_p$, the more uneven the energy flow redistribution caused by power-line and pipeline failures, the more likely it is to cause new failures, so the more critical the power-line and pipeline are.

3.3.2 | Load curtailment severity

As an effective metric to quantify the reliability indices such as loss of load probability (LOLP), loss of load expectation (LOLE), and loss of load frequency (LOLF) in power systems [29], the load curtailment has been utilized widely to characterize the consequence of various failures. In IGPSs, when one power-line or pipeline fails, the power or gas load curtailment could occur to maintain the system operation. Therefore, the load curtailment severity (LCS) metric is developed as another important metric to measure the resiliency of power-lines and pipelines from the point of energy supply reliability. The LCS metrics for power-lines and pipelines are defined as:

$$LCS_k = v\frac{\sum_{i\in I} F^{k}_{\text{LS},i}}{\sum_{i\in I} F_{\text{load},i}} + (1-v)\frac{\sum_{j\in J} P^{k}_{\text{LS},i}}{\sum_{j\in J} P_{\text{load},i}} \tag{44}$$

$$LCS_p = u\frac{\sum_{i\in I} F^{p}_{\text{LS},i}}{\sum_{i\in I} F_{\text{load},i}} + (1-u)\frac{\sum_{j\in J} P^{p}_{\text{LS},j}}{\sum_{j\in J} P_{\text{load},j}} \tag{45}$$

As shown in Equations (44) and (45), the LCS_k and LCS_p respectively reflect the effects of power-line and pipeline failures on gas and power load curtailment from the point of reliability. The larger the LCS_k and LCS_p, the more power and gas load curtailment caused by power-line and pipeline failures, the more critical the power-line and pipeline are.

4 | ASSESSMENT ALGORITHM BASED ON OCWS AND IMPROVED TOPSIS

In this section, the assessment algorithm is designed to synthesize all the metrics proposed in Section 3 to quantify the comprehensive resiliency and detect CPPs. The OCW is first utilized to determine the weight of each metric and the improved TOPSIS method is utilized to quantify the comprehensive resiliency.

4.1 | Weight optimization model for RMs

The evaluation matrix [30] is represented as $R = [r_{\alpha\beta}]_{N\times M}$, where $r_{\alpha\beta}$ denotes the value of metric β for component α; N and M are respectively the numbers of components and metrics. In this paper, the components refer to the pipelines and power-lines, and the metrics are RMs established in Section 3.

The weight of each metric can be obtained by expert preferences-based subjective weighting methods or data characteristics-based objective weighting methods. In order to take both the data characteristics and the preferences of experts into account, the weight optimization model is established to obtain the optimal combination weight (OCW) of each metric.

The weight optimization model is proposed as Equation (46), in which the objective is to minimize the sum of deviation squares between the optimal weights and subjective/objective weights. The subjective weighting method adopts the analytic hierarchy process (AHP) technique and the objective weighting method adopts the criteria importance through intercriteria correlation (CRITIC) method [29].

$$\begin{aligned} &\min \sum_{\beta=1}^{M} \rho_{\text{s},\beta}(w_\beta - \tau_{\text{s},\beta})^2 + \rho_{\text{o},\beta}(w_\beta - \tau_{\text{o},\beta})^2 \\ &\text{s.t.} \quad \rho_{\text{s},\beta} = \tau_{\text{s},\beta}\big/(\tau_{\text{s},\beta} + \tau_{\text{o},\beta}) \\ &\qquad \rho_{\text{o},\beta} = \tau_{\text{o},\beta}\big/(\tau_{\text{s},\beta} + \tau_{\text{o},\beta}) \\ &\qquad \sum_{\beta=1}^{M} w_\beta = 1, \quad w_\beta \ge 0 \end{aligned} \tag{46}$$

where w_β is the OCW of metric β; $\tau_{\text{s},\beta}$ and $\tau_{\text{o},\beta}$ are the subjective weight and objective weight of index β, which are determined by AHP and CRITIC method respectively; $\rho_{\text{s},\beta}$ and $\rho_{\text{o},\beta}$ denote the weighting coefficients of subjective and objective weight of index β.

4.2 | Ranking method based on improved TOPSIS method

The TOPSIS method is an effective technique for ranking and evaluating multi-objective systems [31]. By constructing the "ideal solution" and "negative ideal solution" of multi-objective problems, the relative importance of the schemes can be evaluated by calculating the closeness. However, conventional TOPSIS usually adopts expert weighting methods such as AHP to obtain the weights, which is subjective and arbitrary.

In this paper, an improved TOPSIS method is utilized to rank the resiliency. By solving the weight optimization model in

Equation (46), the OCW of each metric w_β could be obtained, then the weighted resiliency matrix $\mathrm{R}' = [r'_{\alpha\beta}]_{N\times M}$ can be calculated, where $r'_{\alpha\beta} = r_{\alpha\beta} w_\beta$.

The "ideal solution R^+" and "negative ideal solution R^-" are defined respectively as Equations (47)–(50).

$$R^+ = [r_1^+, r_2^+ \cdots, r_\beta^+, \ldots r_M^+] \tag{47}$$

$$R^- = [r_1^-, r_2^- \cdots, r_\beta^-, \ldots r_M^-] \tag{48}$$

where

$$r_\beta^+ = \max\{r'_{1\beta}, r'_{2\beta}, \ldots, r'_{N\beta}\} \quad \beta = 1, 2, \ldots, M \tag{49}$$

$$r_\beta^- = \min\{r_{1\beta}\prime, r_{2\beta}\prime, \ldots, r_{N\beta}\prime\} \quad \beta = 1, 2, \ldots, M \tag{50}$$

The comprehensive resiliency χ_α of each component is defined as:

$$\chi_\alpha = \frac{o_\alpha^-}{o_\alpha^+ + o_\alpha^-} \quad \alpha = 1, 2, \ldots, N \tag{51}$$

where o_α^+ and o_α^- are respectively the Euclidean distance between the $r'_{\alpha\beta}$ and R^+ or R^-, which are expressed as:

$$o_\alpha^+ = \sqrt{\sum_{\beta=1}^{M} (r'_{\alpha\beta} - r_\beta^+)} \tag{52}$$

$$o_\alpha^- = \sqrt{\sum_{\beta=1}^{M} (r'_{\alpha\beta} - r_\beta^-)} \tag{53}$$

As shown in Equations (51)–(53), the comprehensive resiliency χ_α of each component reflects the closeness between the evaluation value and the "ideal solution" and the deviation degree between the evaluation value and the "negative ideal solution". The larger the comprehensive resiliency χ_α, the closer its evaluation value is to R^+ and farther from R^-, and the more critical the component is.

4.3 | Algorithm for identifying CPPs

The flowchart of the proposed method is illustrated in Figure 4 to describe the process for the assessment of the approach.

Furthermore, in order to convey the message in the flowchart to duplicate the proposed approach, the assessment algorithm with the commands is concluded in Algorithm.

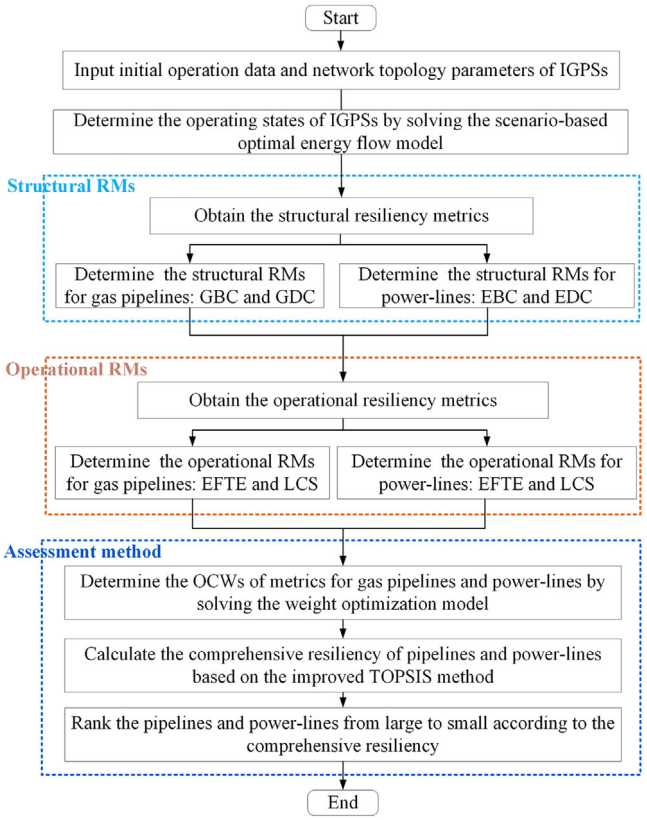

FIGURE 4 Flowchart for resiliency assessment of IGPSs

5 | CASE STUDIES

In order to elaborate the effectiveness of the proposed method, the IEEE 30-bus power system [1] and the Belgian 20-node gas system [27] are modified and combined to compose the test system. As shown in Figure 5, there are seven generating units and 41 power-lines (including three transformer branches) in EPS, and six gas sources (gas wells) and 19 pipelines in NGS. Meanwhile, there are 5 GFUs at electric nodes 5, 7, 8, 11 and 13, whose gas fuels are provided by gas nodes 3, 12, 6, 10 and 15 respectively. On the other hand, the gas sources at gas nodes 1, 2, 5 and 8 depend on power supplies from electric nodes 14, 21, 30 and 26. The remaining units are assumed to be common generating units such as coal-fired units, and other gas sources are powered independently. The capacity of power-lines is equal to 1.5× of power flow in the initial state and set as 15 MW if less than 15 MW. The capacity of pipelines is equal to 1.3× of gas flow in the initial state and set as 5×10^3 m^3/h if less than 5×10^3 m^3/h.

The initial operating state is obtained by solving the OEF model as described in Equations (1)–(20), and the results are shown in Table 1. It can be seen that the installed capacity of GFUs accounted for 47.9% of the total installed capacity, and the output of GFUs accounted for 48.1% of the total output. Obviously, the NGS and EPS are deeply coupled.

5.1 | Calculation results of RMs

The calculation results of RMs proposed in Section 3 are shown in Figures 6 and 7 respectively. It can be seen that the

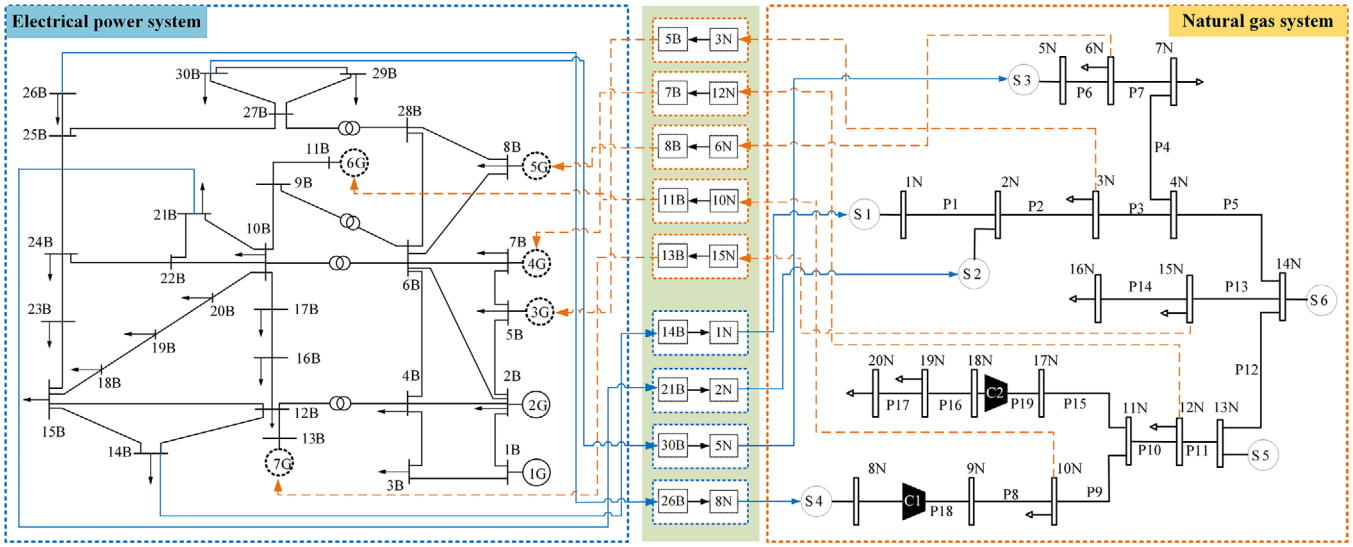

FIGURE 5 Test integrated power and gas systems

ALGORITHM 1 IGPS Resiliency Assessment Algorithm

Input: Network topology parameters of IGPSs, system operation parameters such as generating capacities, and load demands.

Output: Comprehensive resiliency χ_α and CPPs.

for $l = 1$ to N_l **do**
  Remove the pipeline or power-line from the network.
  Calculate the OEF model (1)–(20) based on the updated network, and obtain the l-th operating state of IGPSs.
end for
for $p = 1$ to N_p **do**
  Calculate the structural RMs for pipeline p, including the GBC and GDC metrics as shown in Equations (22) and (25).
  Calculate the operational RMs for pipeline p, including the EFTE and LCS metrics, as shown in Equations (37) and (45).
end for
for $k = 1$ to N_k **do**
  Calculate the structural RMs for power-line k, including the EBC and EDC metrics as shown in Equations (26) and (28).
  Calculate the operational RMs for power-line k, including the EFTE and LCS metrics as shown in Equations (36) and (44).
end for
Calculate the AHP-based subjective weight and CRITIC-based objective weight for each metric.
Calculate the weight optimization model (46) and obtain the OCW of each metric.
Calculate the comprehensive resiliency for pipelines and power-lines based on the improved TOPSIS methods (47)–(53).
Rank the pipelines and power-lines from large to small according to the comprehensive resiliency and detect CPPs.
Return Comprehensive resiliency χ_α and CPPs

TABLE 1 Initial operation state of the test system

Natural gas system			Power system		
Node of sources	Output (m^3/h)	Upper limit (m^3/h)	Bus of units	Output (MW)	Upper limit (MW)
1	17391	17391	1	126.83	150
2	1500	12600	2	20.29	100
5	6995	7200	3	29.08	50
8	33018	33018	7	50.00	50
13	1800	1800	8	6.23	50
14	1440	1440	11	49.07	50
–	–	–	13	1.89	30

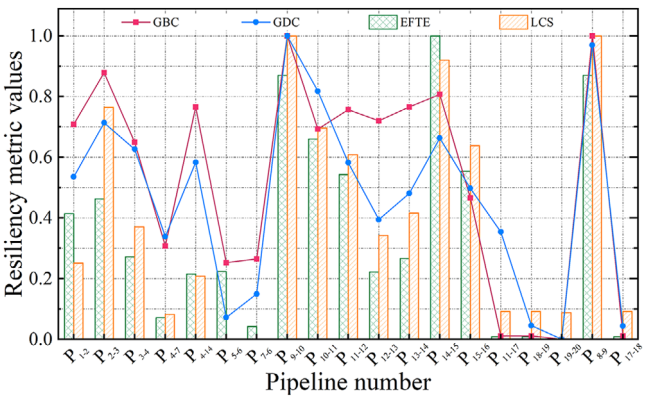

FIGURE 6 Resiliency metric values for pipelines

distribution of different metrics is not completely the same, because they reflect the resiliency from various perspectives.

As shown in Figure 6, the structural RMs including the GBC and GDC metrics of pipelines $P_{1\text{-}2}$ and $P_{4\text{-}14}$ are very large,

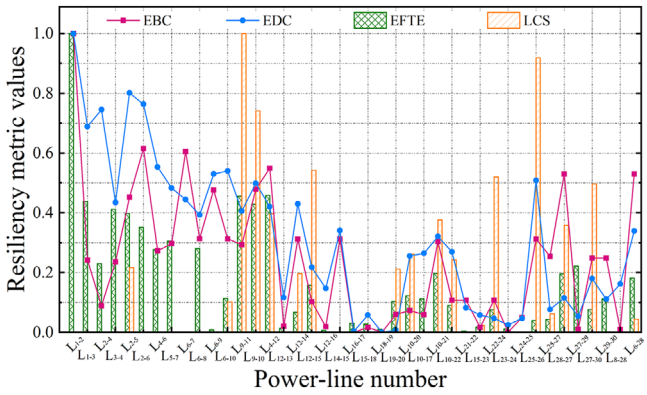

FIGURE 7 Resiliency metric values for power-lines

but operational RMs including the EFTE and LCS metrics are not, meaning that the structural resiliency is more obvious than operation resiliency. It can be seen from Figure 5 that pipelines $P_{1\text{-}2}$ and $P_{4\text{-}14}$ are located in important positions in the network with high degree and betweenness, but the load can be balanced through nearby gas sources after outages, so the failure impact on flow redistribution as well as load loss is not serious. For pipelines $P_{11\text{-}17}$, $P_{17\text{-}18}$, $P_{18\text{-}19}$ and $P_{19\text{-}20}$, the values of four RMs are all small. It can be seen from Figure 5 that pipelines $P_{11\text{-}17}$, $P_{17\text{-}18}$, $P_{18\text{-}19}$ and $P_{19\text{-}20}$ are located at the end of the network and the gas flow through them are very small. So their position in the network is insignificant and the failure impact on system operation is also negligible.

As shown in Figure 7, the EBC metric of power-lines $L_{6\text{-}7}$ and $L_{6\text{-}19}$ is very large since they are located at the outlet of generating units at electric nodes 7 and 11, which are inevitably passed by many shortest paths. However, the power flow through power-lines $L_{6\text{-}7}$ and $L_{6\text{-}19}$ are not large, and the failure impact on flow distribution is also small, so the values of EFTE metric are not high. Power-line $L_{25\text{-}26}$ is located at the end of the EPS network, but the values of LCS metrics are very high. This is because the carried power flow by $L_{25\text{-}26}$ is supplied to the source at gas node 8 that, on removal, would have a great threat to the gas production of NGS. Therefore, power-line $L_{25\text{-}26}$ plays an important role in both network topology and system operation.

5.2 | Identification of CPPs

Based on the calculation results of RMs, the assessment algorithm proposed in Section 4 is employed to calculate the comprehensive resiliency and detect CPPs. The top 5 critical pipelines and power-lines are listed in Table 2 based on different weighting methods.

It can be seen that pipelines $P_{9\text{-}10}$ and $P_{8\text{-}9}$ are the most critical based on the proposed OCWs method, whose four RMs are all very high as shown in Figure 6. It can be seen from Figure 5 that pipelines $P_{8\text{-}9}$ and $P_{9\text{-}10}$ are located in important positions in the network topology with high degrees and betweennesses. Besides, the two pipelines transmit the largest gas flow in the network, reaching 33.018 m^3, and whose removals cause a lot of load curtailment at gas nodes 10, 12, 15 and 16. Therefore, $P_{8\text{-}9}$ and $P_{9\text{-}10}$ are very critical in terms of both topology and reliability.

TABLE 2 Ranking results of CPPs by different methods

	Pipelines				Power-lines			
Rank	Name	OCWs	AHP	CRITIC	Name	OCWs	AHP	CRITIC
1	$P_{9\text{-}10}$	1.00	0.96	1.00	$L_{1\text{-}2}$	1.00	1.00	0.91
2	$P_{8\text{-}9}$	0.99	0.95	0.99	$L_{9\text{-}11}$	0.83	0.69	1.00
3	$P_{14\text{-}15}$	0.93	1.00	0.87	$L_{9\text{-}10}$	0.77	0.64	0.95
4	$P_{10\text{-}11}$	0.74	0.71	0.73	$L_{4\text{-}12}$	0.68	0.62	0.73
5	$P_{11\text{-}12}$	0.64	0.60	0.66	$L_{2\text{-}5}$	0.62	0.53	0.72

As shown in Table 2 and Figure 7, the values of EBC and EDC metrics of power-lines $L_{9\text{-}11}$ and $L_{9\text{-}10}$ are not particularly high but the values of comprehensive resiliency are the second and third largest because of high EFTE and LCS values, validating that the proposed assessment algorithm could integrate multi-dimensional factors to evaluate the comprehensive resiliency.

To validate the effectiveness of the proposed OCW-based weighting method, the results of comprehensive resiliency based on the AHP and CRITIC method are also listed in Table 2. It can be seen from Table 2 that the ranking results based on the three methods are slightly different because of different concerns. For example, the AHP-based method pays more attention to the EFTE metric and the value of pipeline $P_{14\text{-}15}$ is the highest, so $P_{14\text{-}15}$ is ranked the most critical. However, the remaining three metrics of $P_{14\text{-}15}$ are significantly smaller than $P_{9\text{-}10}$ and $P_{8\text{-}9}$, so the results obtained by the AHP-based method are too subjective. Although $P_{14\text{-}15}$ is ranked third by both OCWs-based and CRITIC-based methods, the comprehensive resiliency of $P_{14\text{-}15}$ based on the former method is much larger, showing that the OCWs-based method can take into account both subjective and objective factors.

In order to illustrate the impacts of the integration of NGS and EPS on the resiliency assessment, the distribution of comprehensive resiliency results with and without considering interdependencies are shown in Figures 8 and 9 respectively. An obvious observation is that the integration of NGS and EPS could strengthen the resiliency of pipelines and power-lines located near the coupling infrastructures such as GFUs and EDGSs. Specifically, for the inlet pipelines and outlet power-lines of GFUs, their failures would result in the shortage of power generation or load curtailments in EPS, so the resiliency would increase. For the power-lines connected to nodes that supply power to EDGSs, their malfunction would cause the connected EDGSs to be shut down, further leading to gas load loss. Therefore, the resiliency of these power-lines could be more obvious.

In order to verify the validity of the resiliency results, deliberate attacks and random attacks are carried out on the test system respectively. Deliberate attacks are to disconnect the identified

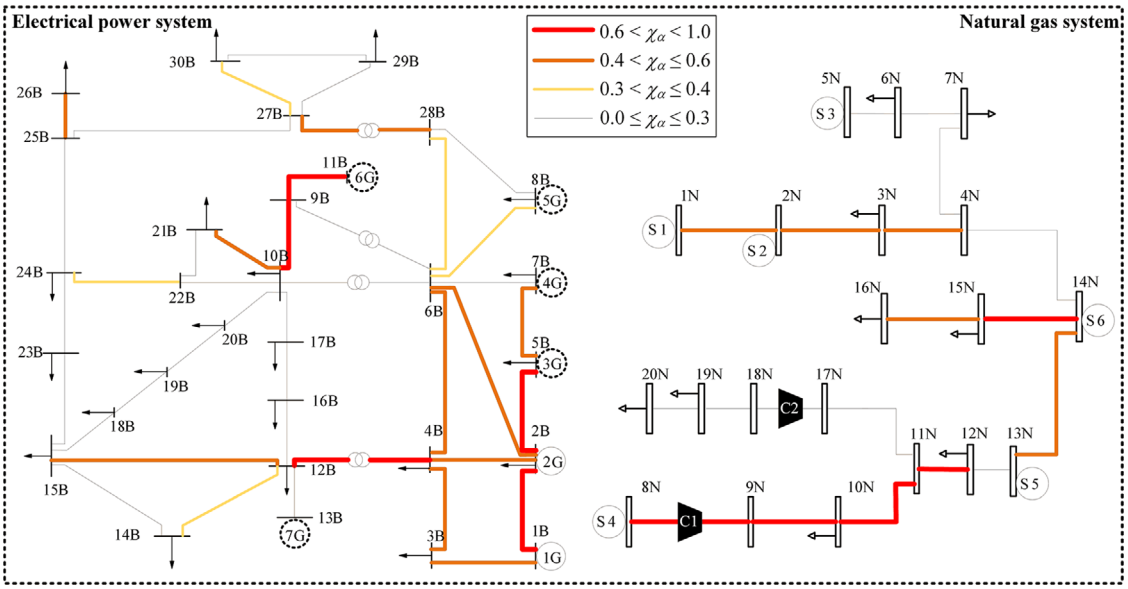

FIGURE 8 Resiliency distribution considering interdependences between EPS and NGS

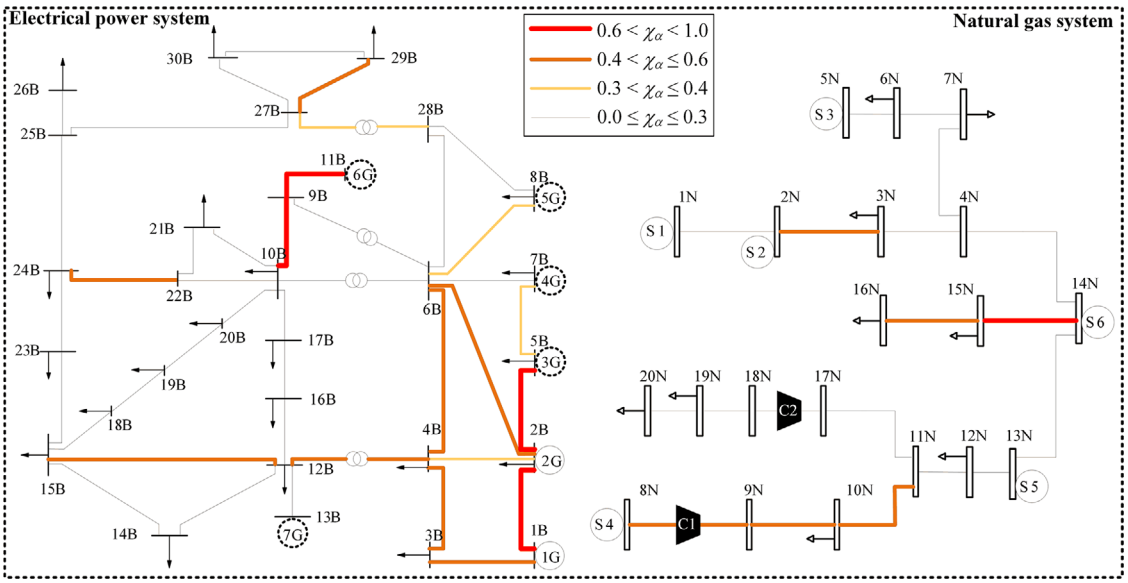

FIGURE 9 Resiliency distribution without considering interdependences between EPS and NGS

CPPs according to their comprehensive resiliency values from large to small, and random attacks are to randomly select the corresponding number of components to attack and the results are averaged by 100×. Besides, to compare the different consequences caused by deliberate attacks and random attacks, two indices are adopted: the residual load and the number of severe components, which are respectively used to quantify the damage from the point of reliability and safety margin. Severe components refer to the pipelines or power-lines carrying energy flow more than 70% of the transmission capacity (i.e. the safety margin is less than 30%). The more severe pipelines or power lines in the system, the smaller the safety margin of the components.

The attack results with respect to the residual load and the number of severe components are shown in Figure 10 and 11 respectively. It can be seen from Figure 10 that the load curtailment caused by deliberate attacks is much larger than random attacks whether in NGS or EPS, indicating that the reliability level of IGPSs is significantly reduced. Specifically, deliberate attacks on six identified critical pipelines quickly reduce the residual gas load to less than 25%, while random attack only reduces the remaining gas load to 70%. For EPS, deliberate attack on ten identified critical power-lines reduces the residual power load to less than 30%, while random attack only causes 20% load loss.

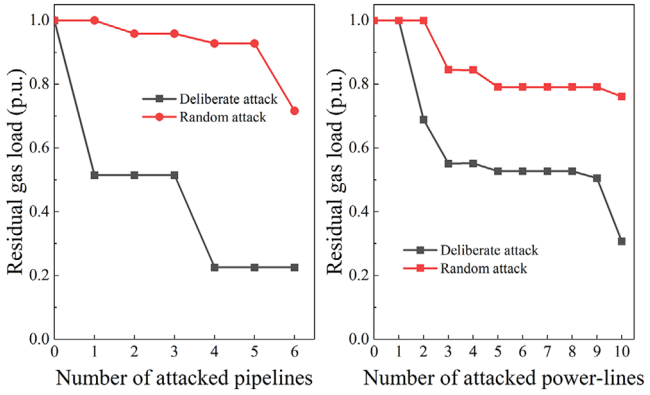

FIGURE 10 Attack results of residual load for NGS and EPS

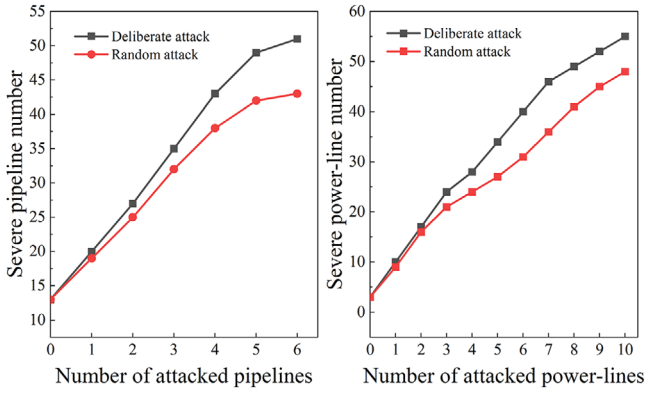

FIGURE 11 Attack results of severe components for NGS and EPS

Moreover, the accumulated number of severe pipelines and power-lines under each deliberate attack is larger than random attacks as shown in Figure 11. In other words, during the deliberate attack process, more pipelines and power-lines carry much energy flow with small safety margin (less than 30% of the transmission capacity), which is more likely to cause further failures due to overloading. As a result, the identified CPPs play a significant role in the safe and reliable operation of IGPSs. Once these CPPs fail due to deliberate attacks, a lot of gas and power load would be shed and the safety margin of components is reduced, bringing great damage to the system. Therefore, operators should focus on protecting the detected CPPs to ensure the safe operation of the system.

5.3 | Comparison under different coupling degrees between NGS and EPS

In order to observe the impact of coupling degrees between NGS and EPS on the resiliency assessment, the installed capacity of common units is reduced from 250 to 100 MW to increase the coupling degree between NGS and EPS. Meanwhile, the installed capacity of GFUs is increased from 230 to 380 MW to keep the total installed capacity of the system unchanged. The initial operation state of the test system in high coupling degree is shown in Table 3. It can be seen that the output of all gas sources is almost at the upper limit, and the proportion of the GFU output to total output is increased from 47.9% to 75.2%.

TABLE 3 Initial operating state of the test system in high coupling degree scenario

Natural gas system			Power System		
Node of sources	Output (m^3/h)	Upper limit (m^3/h)	Bus of units	Output (MW)	Upper limit (MW)
1	17391	17391	1	50.00	50
2	12600	12600	2	20.30	50
5	6623	7200	3	22.59	80
8	33018	33018	7	70.00	80
13	1800	1800	8	10.00	80
14	1440	1440	11	50.51	80
–	–	–	13	60.00	60

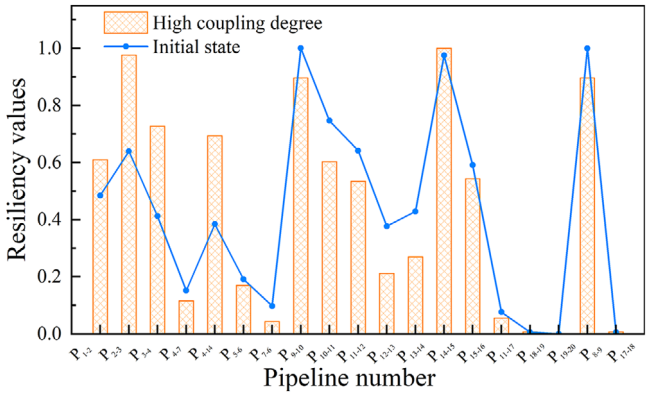

FIGURE 12 Comparisons of pipelines resiliency under different coupling degrees

The comparisons of comprehensive resiliency for pipelines and power-lines between the high coupling degree scenario and original scenario are shown in Figures 12 and 13 respectively. It can be seen from Figure 12 that the resiliency of the pipelines located around the source at gas node 2 such as $P_{1\text{-}2}$, $P_{2\text{-}3}$, and

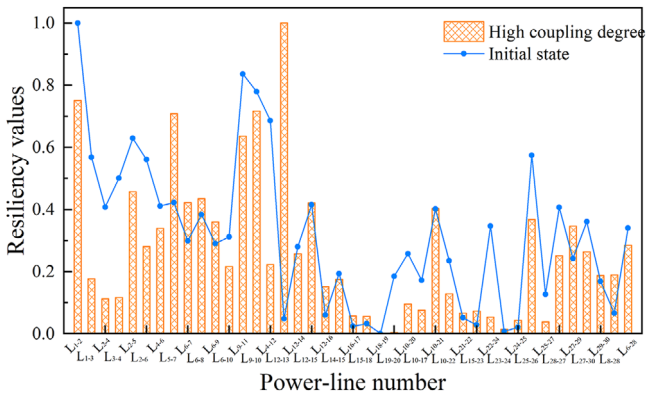

FIGURE 13 Comparisons of power-lines resiliency under different coupling degrees

$P_{3\text{-}4}$ is enlarged because the gas output is increased from 1500 to 12, 600 m^3/h, while other pipeline resiliency changes little because the output of gas sources and gas flow in pipelines change little.

However, the resiliency results of power-lines have more change than pipelines as shown in Figure 13, because the output of generating units change a lot in the high coupling degree scenario. For example, the resiliency of power-lines $L_{1\text{-}2}$, $L_{1\text{-}3}$, $L_{2\text{-}4}$, $L_{3\text{-}4}$ and $L_{2\text{-}5}$ has declined in the high coupling degree scenario because the output of unit at electric node 1 connected with these lines is greatly reduced, from 126.83 to 50 MW, resulting in a decline in the transmission role of these lines. On the contrary, the resiliency of power-lines $L_{5\text{-}7}$, $L_{6\text{-}7}$, $L_{6\text{-}8}$, $L_{6\text{-}9}$ and $L_{12\text{-}13}$ is increased due to the significant increase of GFU output at electric node 7, 8, and 13. Therefore, the resiliency of components located around the coupling infrastructures is more easily affected by the change of coupling degree.

6 | CONCLUSION

In this paper, a novel method for quantifying the resiliency of pipelines and power-lines in IGPSs is put forward. To determine the operation states of IGPSs, a scenario-based optimal energy flow model is proposed and is transformed into a mixed-integer linear programming problem. Then, multi-dimensional RMs in terms of both structural and operational integrity are introduced. Moreover, a new technique synthesizing all the metrics is proposed to quantify the comprehensive resiliency and detect CPPs. Numerical results of case studies show that the proposed method could capture the structure features and operating characteristics as well as the interactions of NGS and EPS, to screen out CPPs effectively. The pipelines and power-lines located in important positions in the network topology or having large impacts on flow redistribution as well as load loss when out of service, show larger resiliency. Besides, the integration of NGS and EPS could strengthen the resiliency of the components that are located near the coupling infrastructures, and the resiliency of power-lines is more easily affected by the integration of NGS and EPS. If the operation operators could protect or strengthen these CPPs pertinently, the system robustness could be greatly improved.

Nomenclature

Abbreviations

AHP	Analytic hierarchy process
CPP	Critical power-lines and pipeline
CRITIC	Criteria importance through intercriteria correlation
EBC	Electrical betweenness centrality
EDC	Electrical degree centrality
EDGS	Electricity-driven gas source
EFTE	Energy flow transfer entropy
EPS	Electric power system
GBC	Gas betweenness centrality
GDC	Gas degree centrality
GFU	Gas-fired unit
IGPSs	Integrated gas and power systems
LCS	Load curtailment severity
NGS	Natural gas system
OCW	Optimal combination weight
OEF	Optimal energy flow
PFTE	Power flow transfer entropy
RM	Resiliency metric
TOPSIS	Technique for order preference by similarity to an ideal solution

Indices and sets

$£_{i,i'}$	Set of shortest paths between gas node i and i'
$\not_{j,j'}$	Set of shortest paths between electric node j and j'
i, i'	Index of gas nodes
I, J	Set of gas nodes/electric nodes
j, j'	Index of electric nodes
$K(j)$	Set of power-lines connected to node j
k, k'	Index of power-lines
$K_1(j), K_2(j)$	Set of power-lines whose initial/terminal node is connected to node j
k_1, k_2	Index of initial/terminal node of power-line k
l	Index of system state sequence
l_0	Initial state
$P(i)$	Set of pipelines connected to node i
P, K	Set of gas pipelines/power-lines
p, p'	Index of gas pipelines
p_1, p_2	Index of initial/terminal node of gas pipeline p
$P_{c1}(i), P_{c2}(i)$	Set of gas active pipelines whose initial/terminal node is connected to node i
p_{c1}, p_{c2}	Index of initial/terminal node of gas pipeline p_c
p_g, p_c	Index of gas passive pipelines/gas active pipelines
P_g, P_c	Set of gas passive pipelines/gas active pipelines
$P_{g1}(i), P_{g2}(i)$	Set of gas passive pipelines whose initial/terminal node is connected to node i
p_{g1}, p_{g2}	Index of initial/terminal node of gas passive pipeline p_g

Variables

$F^l_{sour,i}$	Gas production of gas well at node i and state l
$F^l_{LS,i}$	Gas load curtailment at node i and state l
$F^l_{GFU,i}$	Gas consumption for gas-fired unit at bus i and state l
$f^l_{p_g}$	Gas flow through gas passive pipeline p_g at state l
$\tau^l_{p_c}$	Gas flow through gas active pipeline p_c and state l
π^l_i	Gas pressure square at node i and state l
$P^l_{gen,j}$	Electricity generation of common generating unit at node j and state l
$P^l_{GFU,j}$	Electricity generation of gas-fired unit at node j and state l
$P^l_{LS,j}$	Electricity load curtailment at node j and state l
pf^l_k	Power flow through power-line k at state l
θ^l_j	Voltage phase angle at node j and state l

$y^l_{\text{sour},i}$ State of gas well at node i and state l (binary variable). $y^l_{\text{sour},i} = 1$ if the gas well is normal; $y^l_{\text{sour},i} = 0$ if not.

$z^l_{\text{sour},i}$ Auxiliary continuous variable of gas well at node i and state l

$f^p_{\text{pipe},p'}$ Gas flow of pipeline p' after the outage of pipeline p

$f^k_{\text{pipe},p'}$ Gas flow of pipeline p' after the outage of power-line k

$pf^p_{\text{line},k'}$ Power flow of power-line k' after the outage of pipeline p

$pf^k_{\text{line},k'}$ Power flow of power-line k' after the outage of power-line k

$F^p_{\text{LS},i}$ Gas load curtailment at node i after the outage of pipeline p

$P^p_{\text{LS},j}$ Electricity load curtailment at node j after the outage of pipeline p

$F^k_{\text{LS},i}$ Gas load curtailment at node i after the malfunction of line k

$P^k_{\text{LS},i}$ Electricity load curtailment at node j after the malfunction of line k

Parameters

$C^l_i(\cdot)$ Gas system operation cost function at node i and state l

$C^l_j(\cdot)$ Power system operation cost function at node j and state l

$F_{\text{load},i}$ Gas consumption at node i

$o^m_{i,i'}$ Transmission capacity of the m-th shortest path between node i and i'

$\varsigma^m_{i,i'}(p)$ $\varsigma^m_{i,i'}(p) = 1$ if the m-th shortest path between node i and i' contains pipeline p; $\varsigma^m_{i,i'}(p) = 0$ if not.

$\varkappa_k$ Reactance of power-line k

$o^n_{j,j'}$ Transmission capacity of the n-th shortest path between node j and j'

$\zeta^n_{j,j'}(k)$ $\zeta^n_{j,j'}(k) = 1$ if the n-th shortest path between node j and j' contains power-line k; $\zeta^n_{j,j'}(k) = 0$ if not.

$P_{\text{load},j}$ Power load at node j

G_{HV} Heat value of natural gas

η_{G2P} Conversion efficiency of gas-fired units

η_{P2G} Conversion factor of electricity-driven gas sources

$pf^{\max}_k$ Transmission capacity of power-line k

$F^{\max}_{\text{sour},i}, F^{\min}_{\text{sour},i}$ Upper/lower limit of gas production capacity of gas well at node i

$f^{\max}_p, f^{\max}_{p_g}$ Transmission capacity of pipeline p/passive pipeline p_g

$\pi^{\max}_i, \pi^{\min}_i$ Upper/lower limit of gas pressure square at node i

$\gamma^{\max}_{p_c}, \gamma^{\min}_{p_c}$ Upper/lower limit of compressor ratio of gas active pipeline p_c

$P^{\max}_{\text{GFU},j}, P^{\min}_{\text{GFU},j}$ Upper/lower limit of generation capacity of gas-fired unit at node j

$P^{\max}_{\text{gen},j}, P^{\min}_{\text{gen},j}$ Upper/lower limit of generation capacity of common generating unit at node j

$\theta^{\max}_j, \theta^{\min}_j$ Upper/lower limit of voltage phase angle at node j

M_p, M_{p_g}, M_{p_c} Transmission coefficient of gas pipeline p/passive pipeline p_g/active pipeline p_c

N_l Number of system states

N_p, N_k Number of gas pipelines/power-lines

ACKNOWLEDGEMENTS

This work was supported by National Natural Science Foundation of China (71871200).

REFERENCES

1. Bao, M., et al.: A multi-state model for reliability assessment of integrated gas and power systems utilizing universal generating function techniques. IEEE Trans. Smart Grid. 10(6), 6271–6283 (2019)
2. ERCOT. Review of February 2021 Extreme Cold Weather Event-ERCOT Presentation[R/OL]. http://www.ercot.com/content/wcm/key_documents_lists/225373/Urgent_Board_of_Directors_Meeting_2-24-2021.pdf (2021) access February 24, 2021
3. Department of Energy. Extreme Cold & Winter Weather Hub Situation Update #2[EB/OL]. https://www.energy.gov/sites/prod/files/2021/02/f82/TLP-WHITE_DOE%20Situation%20Update_Cold%20%20Winter%20Weather_%20Report%20%232%20FIN.pdf (2021) access February 17, 2021
4. Yang, Y., Nishikawa, T., Motter, A.E.: Small vulnerable sets determine large network cascades in power grids. Science 358(6365), eaan3184 (2017)
5. Bao, Z., Jiang, Z., Wu, L.: Evaluation of bi-directional cascading failure propagation in integrated electricity-natural gas system. Int. J. Electr. Power Energy Syst. 121, 106045 (2020)
6. Sang, M., et al.: Identification of vulnerable lines in power grid considering impact of natural gas network. Automat Elec. Power Syst. 43(21), 34–43 (2019)
7. Bao, M., et al.: Nodal reliability evaluation of interdependent gas and power systems considering cascading effects. IEEE Trans. Smart Grid. 11(5), 4090–4104 (2020)
8. Zhang, X., Miller-Hooks, E., Denny, K.: Assessing the role of network topology in transportation network resilience. J. Transp. Geogr. 46, 35–45 (2015)
9. Donaldson, D., Alvarez-Alvarado, M., Jayaweera, D.: Power system resiliency during wildfires under increasing penetration of electric vehicles. In: *2020 International Conference on Probabilistic Methods Applied to Power Systems (PMAPS)*, Liege, Benelux, pp. 1–6 (2020)
10. Kim, D., et al.: Network topology and resilience analysis of South Korean power grid. Physica A 465, 13–24 (2017)
11. Sabouhi, H., et al.: Electrical power system resilience assessment: A comprehensive approach. IEEE Syst. J. 14(2), 2643–2652 (2020)
12. Li, B., et al.: A hybrid approach for transmission grid resilience assessment using reliability metrics and power system local network topology. Sustainable Resilient Infrastruct. 6(1–2), 26–41 (2021)
13. Han, F., et al.: Quantifying the importance of elements of a gas transmission network from topological, reliability and controllability perspectives, considering capacity constraints. Risk, Reliability and Safety: Innovating Theory and Practice. CRC, London (2017)
14. Fan, W., et al.: Vulnerable transmission line identification using ISH theory in power grids. IET Gener. Transm. Distrib. 12(4), 1014–1020 (2018)
15. Wang, A., et al.: Vulnerability assessment scheme for power system transmission networks based on the fault chain theory. IEEE Trans. Power Syst. 26(1), 442–450 (2011)
16. Bao, Z., et al.: Analysis of cascading failure in electric grid based on power flow entropy. Phys. Lett. A. 373(34), 3032–3040 (2009)

17. Bompard, E., Napoli, R., Xue, F.: Extended topological approach for the assessment of structural vulnerability in transmission networks. IET Gener. Transm. Distrib. 4(6), 716–724 (2010)
18. Zhu, Y., et al.: Joint substation-transmission line vulnerability assessment against the smart grid. IEEE Trans. Inf. Forensic Secur. 10(5), 1010–1024 (2017)
19. Fang, J., et al.: Power system structural vulnerability assessment based on an improved maximum flow approach. IEEE Trans. Smart Grid. 9(2), 777–785 (2018)
20. Ma, Z., et al.: Fast screening of vulnerable transmission lines in power grids: A pagerank-based approach. IEEE Trans. Smart Grid. 10(2), 1982–1991 (2019)
21. Wei, X., et al.: A novel cascading faults graph based transmission network vulnerability assessment method. IEEE Trans. Power Syst. 33(3), 2995–3000 (2018)
22. Fan, W., et al.: Cascading failure model in power grids using the complex network theory. IET Gener. Transm. Distrib. 10(15), 3940–3949 (2016)
23. Martins, L., et al.: A method for ranking critical nodes in power networks including load uncertainties. IEEE Trans. Power Syst. 31(2), 1341–1349 (2016)
24. Zeng, Z., et al.: Reliability evaluation for integrated power-gas systems with power-to-gas and gas storages. IEEE Trans. Power Syst. 35(1), 571–583 (2019)
25. Wang, S., et al.: Reliability evaluation of integrated electricity-gas system utilizing network equivalent and integrated optimal power flow techniques. J. Mod. Power Syst. Clean Energy 7, 1523–1535 (2019)
26. Nan, L., et al.: Vulnerability identification and evaluation of interdependent natural gas-electricity systems. IEEE Trans. Smart Grid. 11(4), 3558–3569 (2020)
27. Wolf, D., Smeers, Y.: The gas transmission problem solved by an extension of the simplex algorithm. Manage. Sci. 46(11), 1454–1465 (2000)
28. Correa-Posada, C., Sanchez-Martin, P.: Integrated power and natural gas model for energy adequacy in short-term operation. IEEE Trans. Power Syst. 30(6), 3347–3355 (2015)
29. Billinton, R., Allan, N., Reliability evaluation of power systems. 2nd ed., Plenum, New York (1996)
30. Lin, Z., et al.: CRITIC-based node importance evaluation in skeleton-network reconfiguration of power grids. IEEE Trans. Circuits Syst. II-Express Briefs. 65(2), 206–210 (2018)
31. Li, X., et al.: Application of the entropy weight and TOPSIS method in safety evaluation of coal mines. Proc. Eng. 26(4), 2085–2091 (2011)

How to cite this article: Sang, M., et al.: Metrics and quantification of power-line and pipeline resiliency in integrated gas and power systems. IET Gener. Transm. Distrib. 15, 3001–3016 (2021).
https://doi.org/10.1049/gtd2.12236